



NLR-TP-2005-414

## Numerical Simulation of Nonlinear Jet Noise Propagation


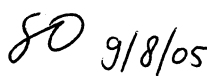

H.H. Brouwer

This report has been based on a paper presented at 11th AIAA/CEAS Aeroacoustics Conference, at Monterey, CA, USA on 23-25 May 2005.

This report may be cited on condition that full credit is given to NLR and the author.

Customer: National Aerospace Laboratory NLR  
Working Plan number: AV.1.H.1  
Owner: National Aerospace Laboratory NLR  
Division: Aerospace Vehicles  
Distribution: Unlimited  
Classification title: Unclassified  
July 2005

Approved by:

Author	Reviewer	Managing department
 9/8/05	 9/8/05	 9/8/05



## Summary

Experimental evidence exists that linear acoustics is inadequate to describe the propagation of high-intensity jet noise. To enable a quantitative assessment of the nonlinear effects, a method has been developed for the numerical simulation of the nonlinear propagation of broadband noise. The method is based on a mixed time-domain/frequency-domain approach to solve the generalised Burgers equation. Application of the method to a single pure tone shows that the results are in agreement with the analytical solution. Subsequent simulations have been carried out of two published experimental tests on jet noise. The computed results for broadband noise satisfy qualitative expectations, i.e. acoustic energy is transferred from the centre frequencies to the higher frequencies. At the high end of the computational frequency domain the computed spectra show anomalous behaviour, which is believed to be a numerical artifact. A quantitative comparison to the experimental results does not yet lead to a conclusive validation.



## Contents

<b>1</b>	<b>Introduction</b>	<b>5</b>
<b>2</b>	<b>Basic equations and solution procedure</b>	<b>6</b>
<b>3</b>	<b>Outline of the algorithm</b>	<b>7</b>
<b>4</b>	<b>Application to a single pure tone</b>	<b>8</b>
<b>5</b>	<b>Application to jet noise</b>	<b>10</b>
5.1	Noise of a F/A-18E/F aircraft	11
5.2	Laboratory experiment on a supersonic jet	14
<b>6</b>	<b>Discussion</b>	<b>16</b>
<b>7</b>	<b>Conclusions and recommendations</b>	<b>17</b>
<b>8</b>	<b>Acknowledgment</b>	<b>18</b>
<b>9</b>	<b>References</b>	<b>18</b>
	1 Table	
	10 Figures	

(19 pages in total)



## Nomenclature

$A$	=	dimensionless diffusivity
$c_0$	=	small-signal speed of sound
$D$	=	nozzle diameter
$f$	=	frequency
$f_s$	=	sample rate
$J_n$	=	Bessel function
$M$	=	index of frequency component with smallest value of $\bar{x}$
$N$	=	number of Fourier coefficients
$P$	=	dimensionless acoustic pressure
Pr	=	Prandtl number
PSD	=	Power Spectral Density
$p$	=	acoustic pressure
$\hat{p}$	=	Fourier transform of acoustic pressure
$R$	=	radial co-ordinate of microphone position
$RHS$	=	right hand side
$r$	=	radial distance
$T$	=	time period of sinusoidal wave
$t$	=	time
$x$	=	distance in one-dimensional problems
$\bar{x}$	=	plane-wave shock formation distance

### Greek:

$\alpha$	=	atmospheric absorption coefficient
$\bar{\alpha}$	=	dimensionless atmospheric absorption coefficient
$\alpha_0$	=	thermoviscous attenuation coefficient
$\beta$	=	dimensionless coefficient of nonlinearity
$\delta$	=	sound diffusivity for a thermoviscous fluid
$\gamma$	=	ratio of specific heats
$\lambda$	=	integer parameter, equals 0 for a one-dimensional problem and 1 for a three-dimensional problem
$\mu$	=	shear viscosity
$\mu_B$	=	bulk viscosity
$\nu$	=	kinematic viscosity
$\theta$	=	dimensionless retarded time
$\rho_0$	=	density of air
$\sigma$	=	dimensionless distance
$\tau$	=	retarded time
$\omega$	=	angular frequency

### subscripts:

0	=	reference
$rms$	=	root-mean-square
$s$	=	source



## 1 Introduction

It is common practice to determine the noise impact of aircraft (both civil and military) by using computations, rather than by measurements. Noise impact computations usually make use of noise levels, measured at a relatively small distance from the aircraft, combined with a propagation model. These propagation models are based on linear acoustics and account for effects like atmospheric absorption and lateral attenuation.

In the past decades however, evidence has been found that linear acoustics is inadequate to describe the propagation of high-intensity jet noise, as generated by fighter aircraft like the F-22 or the F/A-18<sup>1</sup>. More specifically, it is found that the high frequency part of the spectrum is decaying much slower than predicted by linear acoustics. This behaviour is generally attributed to nonlinear effects in the propagation. However, it seems that no suitable computation method has been found yet, to confirm this hypothesis, or to account for these effects in environmental noise impact models.

It is generally accepted that the (generalised) Burgers equation for the acoustic pressure is the appropriate equation to analyse the nonlinear propagation of sound (e.g. Ref. 2). In the case of the original, one-dimensional Burgers equation, analytical approximations are known for an initial sinusoidal waveform. No such solution is known, however, for the generalised Burgers equation, which incorporates 3-dimensional spherical spreading. A second, even more complicating aspect of jet noise is that a main component of it (in the case of subsonic jets the only significant one) is mixing noise. This broadband noise is generated by stochastic, turbulent processes, and solutions for deterministic, periodic time signals seem useless for this application.

Therefore, most prediction methods are focused on the Power Spectral Density (PSD), a quantity that contains meaningful time-averaged spectral information, but no phase information. The PSD is usually the quantity in which experimental results are reported. For the PSD, being the Fourier transform of the second order moment of the pressure time signal, an equation can be derived by using the Burgers equation for the pressure. However, in the right hand side of this equation a third order moment appears, which again can be inserted into the Burgers equation, leading to a right hand side with a fourth order moment. By continuation of this scheme an infinite hierarchy of equations is obtained. In some papers the analysis is based on a truncated series, but it appears that such a series cannot predict the nonlinear propagation over longer distances<sup>3</sup>. In reference 4 an attempt is made to remedy this shortcoming by transforming the second term of the series into a new differential equation, valid for the whole domain. In this approach it is assumed that the initial signal is Gaussian, and stays almost Gaussian. Another method has been proposed recently by Menounou and Blackstock<sup>5</sup>. Their approach is based on including ever-higher order moments, all evaluated at the source, while marching the numerical solution forward along the spatial variable. At present their model does not incorporate



spherical spreading nor atmospheric absorption. Furthermore it can only be used if the moment of any order can be evaluated at the source. The authors give two examples where this is possible: a sinusoidal waveform and a Gaussian stochastic process. It is not clear yet to which extent the latter process can adequately represent jet noise.

In the present paper a method is described that is based on a mixed time-domain/frequency-domain approach for a simulated time signal. In principle the method can also be used with a measured time series as input, but it is assumed here that only an initial (source) PSD is known. By using a time signal, be it a measured one or a simulated one, no assumptions are needed with respect to the higher order averaged moments of the acoustic pressure. The way in which the data, representing a pressure time series, are handled in the presented method is similar to the way measured data are handled in digital signal processing.

In section 2 of the report the basic equations are derived and the solution method is explained. This method is implemented in an algorithm, an outline of which is given in section 3. The application to a simple sinusoidal waveform and comparison with the analytic solution is presented in section 4. The results of the application to two jet noise experiments are presented in section 5. Some aspects of the method and the results are discussed further in section 6. Finally, conclusions and recommendations are given in section 7.

## 2 Basic equations and solution procedure

In references 2 and 6 it is shown that the weakly nonlinear propagation of acoustic waves is described by the Burgers equation. ‘Weakly nonlinear’ means here that terms of the relative order of  $(u_0/c_0)^2$  are neglected, where  $u_0$  is the velocity amplitude of a plane wave and  $c_0$  is the small-signal speed of sound. In reference 6 it is argued that for a plane wave the relative error is less than 0.5% at a sound level of 154 dB.

The (one-dimensional) Burgers equation is given by:

$$\frac{\partial p}{\partial x} = \frac{\beta p}{\rho_0 c_0^3} \frac{\partial p}{\partial \tau} + \frac{\delta}{2c_0^3} \frac{\partial^2 p}{\partial \tau^2} \quad (1)$$

where  $p$  is the acoustic pressure,  $x$  the spatial variable,  $\beta$  the coefficient of nonlinearity,  $\rho_0$  the ambient density of air,  $\tau = t - x/c_0$  is the retarded time, and  $\delta$  is the sound diffusivity for a thermoviscous fluid. Equation (1) does not include spherical spreading nor the absorption by molecular relaxation. A generalised form of the Burgers equation that does include these effects is given by:

$$\frac{\partial p}{\partial r} + \frac{\lambda}{r} p = \frac{\beta p}{\rho_0 c_0^3} \frac{\partial p}{\partial \tau} + \frac{\delta}{2c_0^3} \frac{\partial^2 p}{\partial \tau^2} - \alpha p \quad (2)$$



where  $r$  is the radial distance and  $\alpha$  is the atmospheric absorption coefficient. The parameter  $\lambda$  equals 0 for a one-dimensional problem and 1 for a three-dimensional problem. To solve this equation we follow a procedure outlined in reference 6, pp. 312-314. Note that details, e.g. in the scaling, may not be the same. First, we introduce the following dimensionless variables:

$$P = p / p_0, \quad \sigma = r / \bar{x}, \quad \theta = \omega_0 \tau, \quad A = \alpha_0 \bar{x}, \quad \bar{\alpha} = \alpha \bar{x} \quad (3)$$

where  $p_0$  is a reference pressure,  $\omega_0$  a reference angular frequency,  $\bar{x} = \rho_0 c_0^3 / \beta p_0 \omega_0$  is the lossless plane-wave shock formation distance for a signal with source condition  $p = p_0 \sin(\omega_0 t)$ , and  $\alpha_0 = \delta \omega_0^2 / 2c_0^3$  the thermoviscous attenuation coefficient at frequency  $\omega_0$ . Substituting this into Eq. (2) we find:

$$\frac{\partial P}{\partial \sigma} = -\frac{\lambda}{\sigma} P + P \frac{\partial P}{\partial \theta} + A \frac{\partial^2 P}{\partial \theta^2} - \bar{\alpha} P \quad (4)$$

To solve Eq. (4) we assume that the pressure can be written as a finite Fourier sum:

$$P(\sigma, \theta) = \sum_{n=-N}^N P_n(\sigma) e^{in\theta/M} \quad (5)$$

The integer number  $M$  (which is not present in reference 6) is introduced because we intend to apply the method to broadband noise. The frequency resolution determined by Eq. (5) should be much smaller than the frequencies of main physical interest (i.e.  $\Delta\omega \ll \omega_0$ ), which necessitates the factor  $M$ . The way this factor is determined in practice, will become clear in the sequel. Note that  $P_{-n} = P_n^*$ , where  $*$  denotes complex conjugate, because  $P$  is real. Substitution of Eq. (5) into Eq. (4) and rearranging terms according to reference 6 yields:

$$\frac{dP_n}{d\sigma} = -\left(\frac{\lambda}{\sigma} + \frac{n^2}{M^2} A + \bar{\alpha}\right) P_n + i \frac{n}{2M} \left( \sum_{m=1}^{n-1} P_m P_{n-m} + 2 \sum_{m=n+1}^N P_m P_{m-n}^* \right) \quad (6)$$

where it is assumed that  $P_0$  (the time-averaged pressure) vanishes.

So we end up with  $N$  coupled ordinary differential equations. In the next section the algorithm is described with which this system is solved numerically.

### 3 Outline of the algorithm

Input to the algorithm is a pressure time series, i.e. a set of pressure values (samples)  $p_j$ , in Pascal, denoting the pressure values at a given sample rate  $f_s$  (in  $s^{-1}$ ), i.e.  $p_j = p(t_j)$  with  $t_j = j/f_s$ . First, the largest number (smaller than the total number of samples) is determined which is a power of 2, in order to enable the use of Fast Fourier Transforms (FFT's). The result determines



the number  $N$ , introduced in the previous section. Note that the maximum frequency in the system is given by  $f_s/2$ , and the frequency resolution by  $\Delta f = f_s/N$ , which are relations well-known from digital signal analysis. The reference pressure  $p_0$  is set to  $\sqrt{2}p_{rms}$  where the root-mean-square value is determined by:

$$p_{rms} = \frac{1}{N} \sqrt{\sum_{j=1}^N p_j^2} \quad (7)$$

Next an FFT routine is applied to the time series, yielding the complex amplitudes of the  $N/2$  frequency components. The reference parameter that reflects the level of nonlinearity, is the lossless plane-wave shock formation distance  $\bar{x}$ . If there is no nonlinearity this parameter is infinite. In the algorithm the value of  $\bar{x}$  is determined for each frequency component, with the corresponding amplitude as reference pressure (note that summing the positive and negative frequency terms yields a real value). Out of this set of  $N/2$  values for  $\bar{x}$ , the smallest one is selected; the corresponding index is chosen as  $M$ , and the corresponding frequency determines  $\omega_0$  (see previous section). This procedure ensures that, if the input signal is a single pure tone, it satisfies  $p = p_0 \sin(\omega_0 t)$  (apart from a possible phase shift) and  $\bar{x}$  satisfies its original definition. Now we have determined all the reference parameters necessary to make the equations dimensionless.

Also input to the algorithm is a step size  $\Delta\sigma$ . At each step in  $\sigma$ , the right hand side of Eq.(6), denoted here by  $RHS_n(\sigma)$ , is determined for  $n=1,2,3,\dots,N/2$  successively, by using the *current* values of  $\{P_n\}$ . Before moving to  $n+1$ , the new value of  $P_n$  is determined by  $P_n = P_n + \Delta\sigma \times RHS_n(\sigma)$ . This means that in the calculation of  $RHS_n(\sigma)$ , the new values of  $P_m$  are used if  $m < n$ , whereas the old values are used if  $m \geq n$ . This amounts to the application of an *explicit* Euler scheme at the low-frequency end ( $n=1$ ), gradually evolving into an *implicit* Euler scheme at the high-frequency end ( $n=N/2$ ). This integration procedure, and alternatives, will be discussed further in section 6.

Stepping from a given initial value of  $\sigma$  to a given end value, results into the final Fourier coefficients  $P_n$ , which can be transformed again, if desired, into a pressure time series.

#### 4 Application to a single pure tone

Before we can apply the method we have to determine the constants  $\beta$  and  $\delta$ . From reference 6 we have  $\beta = (\gamma + 1)/2$ , with  $\gamma$  the ratio of specific heats, which yields  $\beta = 1.2$  for air. Further:

$$\delta = \nu \left( \frac{4}{3} + \frac{\mu_B}{\mu} + \frac{\gamma - 1}{Pr} \right) \quad (8)$$



where  $\nu$  is the kinematic viscosity,  $\mu_B$  the bulk viscosity,  $\mu$  the shear viscosity, and  $Pr$  is the Prandtl number. For standard atmospheric conditions we find  $\delta = 3.64 \times 10^{-5}$ . In this section the atmospheric absorption is neglected.

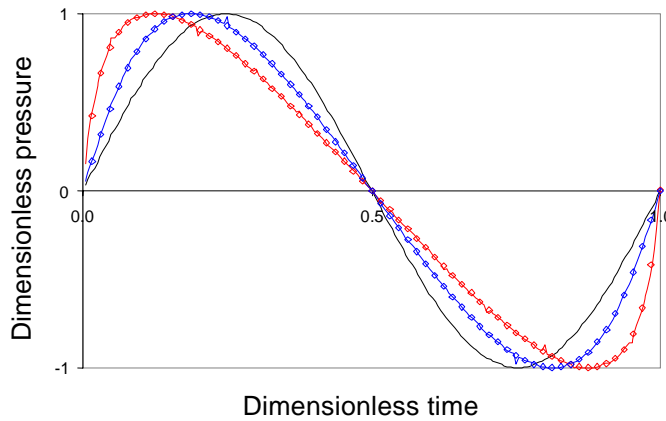
The following input time series has been constructed:

$$p_j = p_0 \sin(2\pi f_0 t_j), \quad t_j = j / f_s, \quad j = 1, 2, \dots, N, \quad (9)$$

with  $p_0 = \sqrt{2} \times 200$  Pa (SPL = 140 dB),  $f_0 = 750$  Hz,  $f_s = 48000$ , and  $N = 8192$ . With these input data, one-dimensional computations ( $\lambda = 0$ ) were carried out, from  $\sigma = 0$  to  $\sigma = 0.4$  and  $\sigma = 0.8$  respectively. The results have been compared with an analytic approximation from reference 2 (Fubini solution):

$$P(\sigma, \theta) = 2 \sum_{n=1}^{\infty} \frac{J_n(n\sigma)}{n\sigma} \sin(n\theta) \quad (10)$$

In figure 1 the results for  $P$  are plotted as function of  $\tau/T$  where  $T$  is the time period of the input signal.



*Fig. 1 Results for a single pure tone, — input signal,  
 ◆  $\sigma = 0.4$  present method, —  $\sigma = 0.4$  analytic,  
 ◆  $\sigma = 0.8$  present method, —  $\sigma = 0.8$  analytic*

As the curves computed with the present method and those computed from Eq.(10) are hardly discernible from each other, it can be concluded that the method presented here works well for the values of  $\sigma$  considered. For higher values of  $\sigma$  however, i.e. as  $\sigma$  approaches unity, the results behave irregularly near  $\tau/T = 0$  and  $\tau/T = 1$ , see e.g. the results for  $\sigma = 0.98$  in figure 2.

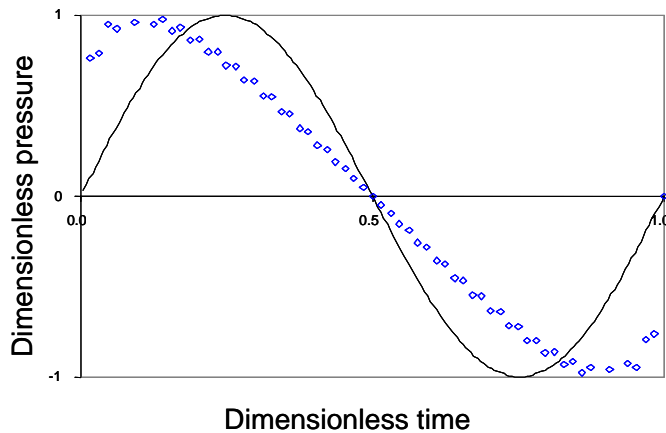


Fig. 2 Results for  $\sigma = 0.98$

For  $\sigma = 1$  the exact solution is an N-wave, with discontinuities at  $\tau/T = 0$  and  $\tau/T = 1$ . A Fourier sum is not a suitable representation of such a function.

## 5 Application to jet noise

In this section the method outlined in the section 3 will be applied to two experiments, firstly to the one reported in reference 1, on the noise of a jet fighter, and secondly to the one of reference 7, on the noise of a supersonic jet in a laboratory experiment. In both cases a measured time series, needed as input of the algorithm, was not available to the author. Therefore, a broadband time signal is constructed, starting from the published Power Spectral Density, written as  $\text{PSD}_s(f)$ . The objective thus is to construct a time series of  $N$  samples corresponding to a sample rate  $f_s$ , the Power Spectral Density of which equals  $\text{PSD}_s(f)$ . This is achieved in the following steps:

- A sequence of  $N$  random numbers satisfying a Gaussian distribution with zero mean and unit variance is generated. This sequence represents band-limited white noise.
- This white noise time series is Fourier-transformed.
- The Fourier coefficients are scaled to the starting spectrum  $\text{PSD}_s(f)$ .
- By application of an inverse Fourier transformation, a broadband time signal is obtained with the desired PSD.



### 5.1 Noise of a F/A-18E/F aircraft

In reference 1 an experiment on the noise of an F/A-18E/F aircraft is presented. In this experiment noise data were acquired at distances of 18 m, 74 m, and 150 m from the nozzle of this aircraft, during a static engine run-up test. In figure 3, copied from reference 1, measured data are shown from the microphone at 18 m.

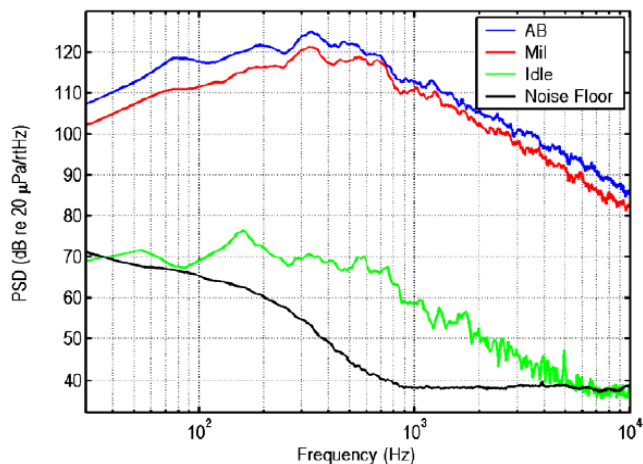


Fig. 3 PSD of F/A-18E/F noise at 18 m (from reference 1)

The data taken at military thrust, indicated by ‘Mil’ will be simulated by use of the procedure described above. Instead of trying to reproduce the PSD in figure 3 in detail, it is observed that the low frequency part of the spectrum behaves as  $f^{1.7}$ , whereas the high frequency part behaves as  $f^{-2.7}$ .

Therefore, the following approximation for the PSD was adopted:

$$\text{PSD}_s(f) = 10^{10} \log \left( \frac{2.5 \times 10^{19} f^{1.7}}{4.21 \times 10^{11} + f^{4.4}} \right) \quad (11)$$

with  $f$  in Hz. With this function as input, a time signal was generated, using the procedure described above, with the following parameters:  $N = 2^{16}$ ,  $f_s = 2^{16} \text{ s}^{-1}$ , leading to a time record of 1 s, a frequency resolution of 1 Hz, and a maximum analysis frequency of 32768 Hz. The results for the simulated input PSD and the narrowband frequency spectrum of the simulated time signal are shown in figure 4, where the narrowband data have been averaged over 16 blocks of 2048 data, resulting in frequency bands of  $\Delta f = 16 \text{ Hz}$ . The Overall Sound Pressure Level (OASPL) of the simulated time signal is 148 dB, close to the measured result 147 dB.

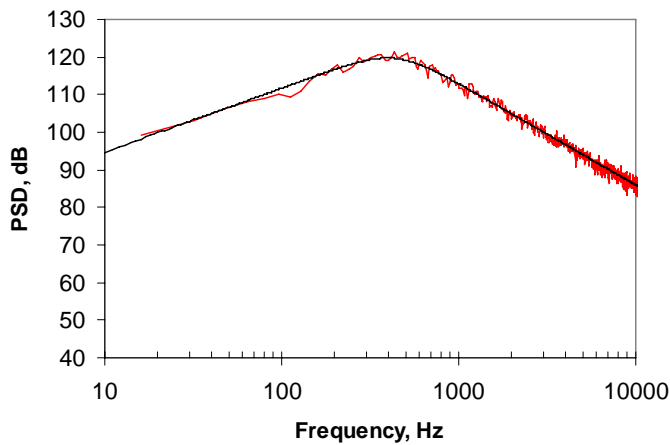


Fig. 4 Input PSD (—) and simulated narrowband spectrum (—•—),  $\Delta f = 16$  Hz

In figure 5 the Probability Density Function (PDF) of the simulated data is compared to a Gaussian distribution, showing that only very small deviations occur. This means that scaling the white noise spectrum to the measured spectrum does not affect the Gaussian statistics. Note that in reference 1 a skewness (which is a measure of the asymmetry of the PDF) of 0.38 is reported.

Skewness is associated with the phenomenon of crackle. In reference 7 it is stated that if the skewness value is below 0.3, the signal is crackle-free, whereas for skewness values higher than 0.4 the signal contains significant crackle. In the present report no attempt is made to simulate crackle.

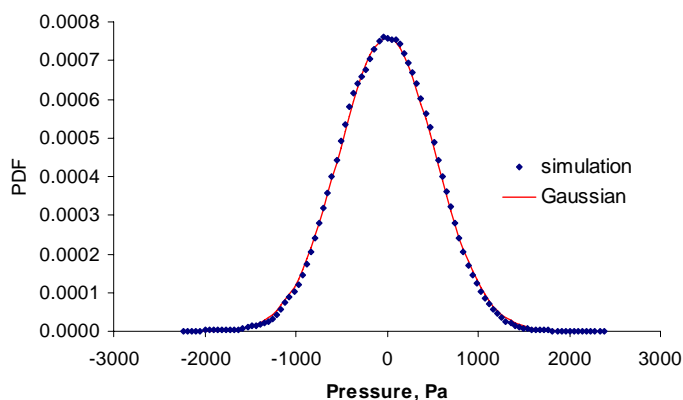


Fig. 5 Probability Density Function of simulated time signal compared to Gaussian distribution

The time signal is fed into the computer program outlined in section 3, with  $r = 18$  m as starting point and  $r = 150$  m as end point. The atmospheric absorption coefficients are determined according to the method by Bass et al. (Refs. 8 and 9). The step size is set at  $\Delta\sigma = 0.005$ . The



value for  $\bar{x}$  returned by the program is 16.9 m, so 1562 steps are required, each step taking about 7.5 s on a standard PC (2 GHz, 1 GB of RAM).

Before presenting the results, we first copy in figure 6 a figure from reference 1, showing the spectrum measured at 150 m, together with results from a linear extrapolation from the data taken at 18 m, and with results predicted with the models of references 3 and 4.

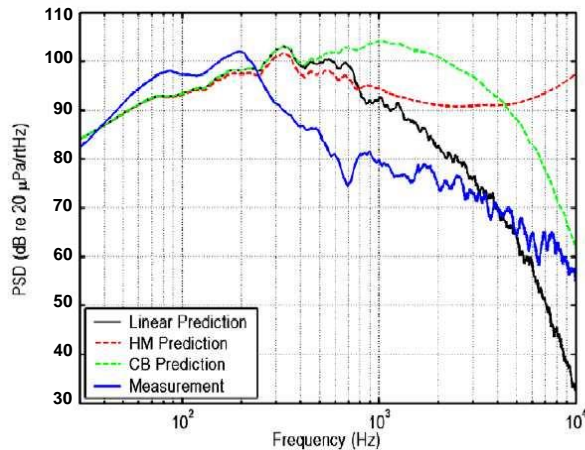


Fig. 6 Measured and predicted data from reference 1. CB refers to reference 3, HM to reference 4

The results from the present method are shown in figure 7, with a frequency resolution of  $\Delta f = 32$  Hz.

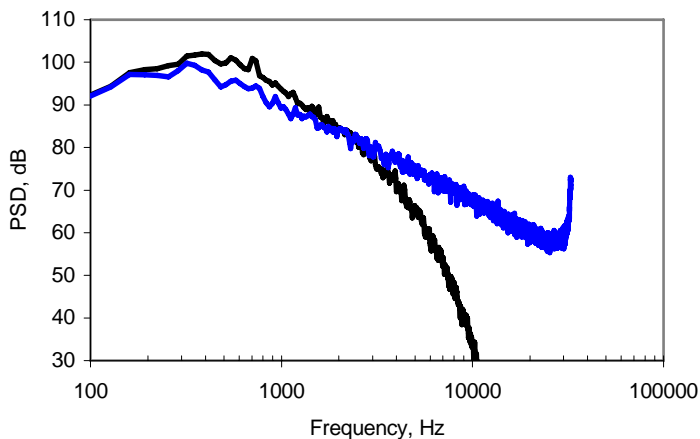


Fig. 7 Results of the present method

The black curve ('Linear prediction') is obtained with the same computer program, with the nonlinear terms switched off. One of the remarkable features in this figure is the sharp rise in



the nonlinear prediction at the high end of the spectrum. By variation of the sample rate and the frequency resolution it has been assessed that this rise always occurs at about 85% of the maximum frequency, and should be regarded as an artifact, caused by the finiteness of the frequency domain considered. It looks as if the acoustic energy that is transferred from the centre frequencies to the higher frequencies, gets stuck at the end of the domain, and is accumulated there. Apart from this artifact, the (averaged) results do not change significantly with variation of the sample rate or the frequency resolution.

Comparing figure 7 to figure 6, we see that the measured data are not reproduced accurately in a quantitative sense, but the effects attributed to nonlinear propagation are qualitatively the same in both figures: acoustic energy is transferred from the centre frequencies to the higher frequencies, leading to a significantly lower decay of this part of the spectrum. It is clear that the present method does a much better job than the methods of Refs. 3 and 4.

Whether the quantitative differences are due to deficiencies of the method or are caused by the way the measurements were carried out (e.g. ground reflection), is not evident at present. Also the PDF of the results of the nonlinear prediction method has been computed, see figure 8.

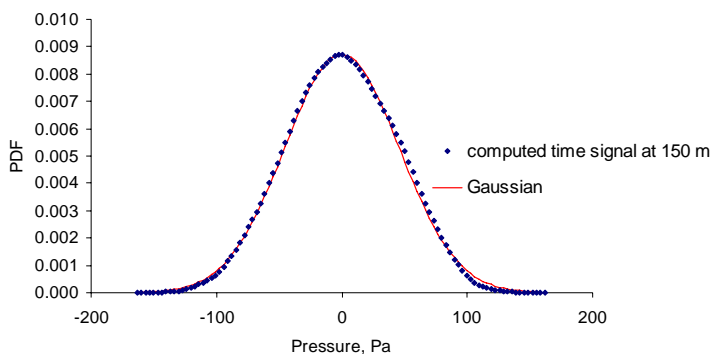


Fig. 8 PDF of computed time signal at 150 m

From this result it seems that the nonlinear propagation process does not significantly affect the Gaussian statistics.

## 5.2 Laboratory experiment on a supersonic jet

In reference 7 experiments on a supersonic jet with a nozzle diameter of  $D = 12.7$  mm are reported. The measurements were carried out in an anechoic chamber. Microphones were mounted at distances of  $R/D = 15, 30, 60,$  and  $100$ . Both cold and hot jets were tested, hot jets being simulated by feeding helium into the air stream. Only the hot jets produced noise levels high enough to exhibit nonlinear effects over short distances. In figure 9 the main acoustic results are shown, as Sound Power Levels plotted against Strouhal number.

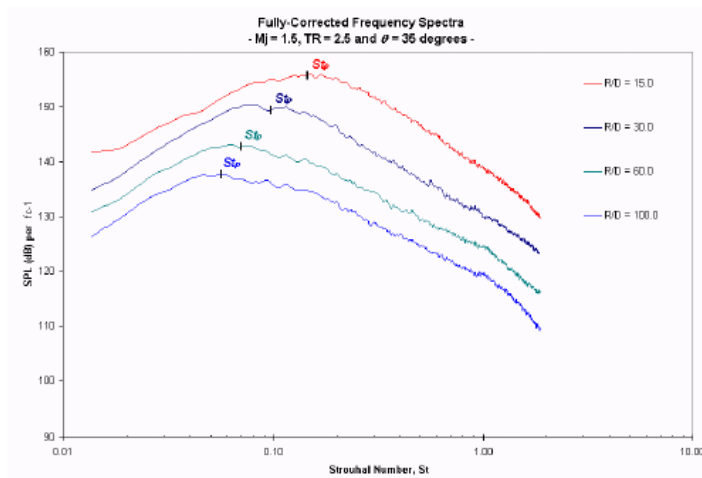


Fig. 9 Spectra measured at 4 distances from a supersonic, hot jet (Ref. 7)

A time signal has been constructed in the same way as above, with the parameters:  $N = 2^{16}$ ,  $f_s = 301466 \text{ s}^{-1}$ , leading to a time record of 0.217 s, a frequency resolution of 4.6 Hz, and a maximum analysis frequency of 150 kHz. As the experimental results were corrected for atmospheric absorption, this effect was not incorporated in the simulation. The step size is now set at  $\Delta\sigma = 0.01$ . The value for  $\bar{x}$  returned by the program is 0.25 m.

The results from the present simulation method for the same distances are presented in figure 10.

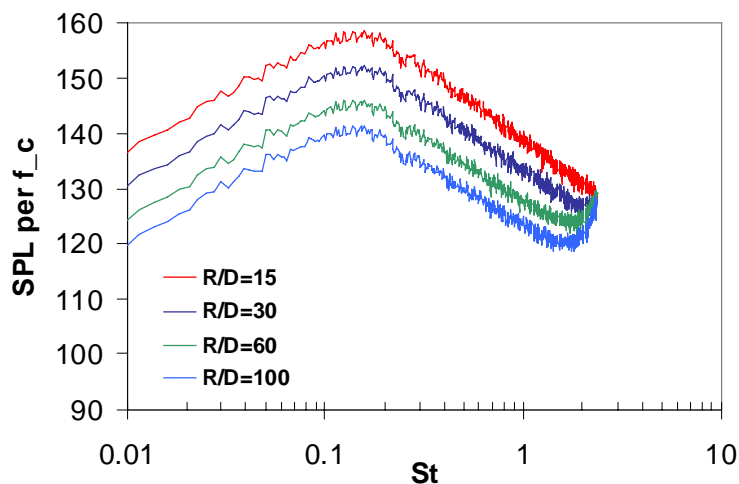


Fig. 10 Computed spectra for the case of reference 8

The main difference between the measured and computed results is that in the measurements the centre frequencies are attenuated much faster, leading to both lower peak levels and a shift of the peak frequency to lower values. Also the slope of the spectra at high frequencies is not changing at the same rate in the computed results as in the measured ones, see Table 1.

*Table 1 Attenuation rate for high frequencies in dB per decade*

Freq. attn. (dB/decade)	$R/D = 15$	$R/D = 30$	$R/D = 60$	$R/D = 100$
Measurements (Ref. 7)	26.3	22.5	19.3	18.1
Simulation	26.3	23.7	22.5	21.5

The cause of these differences is not known at the moment of writing. A possible explanation might be that in the experiments a significant amount of crackle was observed, with a skewness value of 0.73 at  $R/D = 15$ . Although crackle is a source phenomenon, and not associated with non-linear propagation, it should not be excluded that the combination of both effects will significantly change the results. This will be the subject of future investigations.

## 6 Discussion

The comparison of the results of the method presented in sections 2 and 3 with experimental results, does not lead to a conclusive validation. This might be caused by effects in the experiments which are not incorporated in the model (such as ground reflection in the case of section 5.1) or misinterpretation of the experimental results (section 5.2). With respect to the latter case, some of the required data are not given in reference 7 and have to be estimated, such as the jet velocity, required for the translation from frequency to Strouhal number.

On the other hand, the simulation model also has some limitations, one of which is the finite number of Fourier coefficients ( $N/2$ ). A consequence of this limitation is that discontinuities are not modeled adequately. As explained in section 4, nonlinear propagation leads to the formation of shock waves (or N-waves), which are not represented accurately by a Fourier decomposition. In both cases considered in section 5, the range of simulation was far greater than the typical plane-wave shock formation distance. It is conjectured however, that if the maximum frequency in the simulation sufficiently exceeds the maximum frequency of interest, the results will be fairly reliable. Discontinuities mainly affect the high frequency components and it may be expected that the exchange of acoustic energy between the lower frequency components is modeled well by the present method. Whether the sharp rise at the high end of the spectrum, as shown in figure 7 and figure 10, can be attributed to the poor representation of N-waves has not been verified yet. For an analysis of the waveform near or beyond the shock formation distance, the present method is thus not suitable.

The effect of a finite number of Fourier coefficients has been investigated by varying  $N$  and the sample rate  $f_s$ . As an example, in figure 11 the results of figure 7, obtained with a sample rate of  $f_s = 65536$ , are shown again, now together with results obtained with the same number of samples, but with a sample rate of 5 times as high,  $f_s = 327680$ .



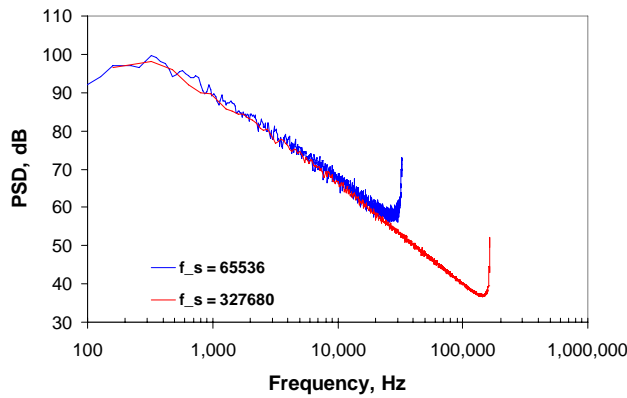


Fig. 11 Results for the case of section 5.1, for two different sample rates

The differences between the two curves, apart from the high end of the spectrum, do not exceed the statistical fluctuations.

In section 3 it is explained that the integration procedure used, is effectively an explicit (Euler) procedure for the low frequencies and an implicit procedure for the high frequencies. The reason to use this procedure initially, was that it is the easiest procedure to implement in a computer program. Some effort has been spent on finding faster alternatives. First a completely explicit procedure was tried, i.e. the right hand side of Eq. (6) is computed for each  $n$  (using the values of  $\{P_n\}$  from the previous step), after which the solution is marched one step forward. This method, however, proved to be unstable, at least for time steps comparable to those used in the first method. Apparently the system of differential equations has a ‘stiff’ character, and the solution requires application of a (semi-)implicit method. The use of more sophisticated methods, like Runge-Kutta, is more complicated for implicit methods than it is for explicit methods, and has not been considered any further.

The largest possible step size (i.e.  $\Delta\sigma$ ) used in the present method is assessed by trial and error. Consistency of the method has been checked by application of several different step sizes.

## 7 Conclusions and recommendations

In this report a method is presented for the numerical simulation of the nonlinear propagation of broadband noise. The method is based on a mixed time-domain/frequency-domain approach. Simulations have been carried out of two published experimental tests on jet noise.

The main conclusions are:

- The presented method works well for a single pure tone.



- The results for broadband noise satisfy qualitative expectations, i.e. acoustic energy is transferred from the centre frequencies to the higher frequencies.
- The computed spectra show anomalous behaviour at the high end of the computational frequency domain.
- Comparison to experimental results does not lead to a conclusive validation. The occurrence of crackle in one of the tests may be a cause for deviations.

The following future investigations are recommended:

- Find additional test cases for validation.
- Investigate the high-frequency part of the results and the connection with N-waves.
- Include crackle in the simulations.
- Use simulations to assess the effect of nonlinear propagation on environmental impact computations.

## 8 Acknowledgment

This research was partly funded by the Royal Netherlands Air Force, contractnumber 135-04-0401-11.

## 9 References

- 1 Gee, K.L., Gabrielson, T.B., Atchley, A.A., and Sparrow, V.W., "Preliminary Analysis of Nonlinearity in F/A-18E/F Noise Propagation", AIAA Paper 2004-3009, June 2004.
- 2 Crighton, D.G., "Model Equations of Nonlinear Acoustics", *Annual Review of Fluid Mechanics*, Vol.11, January 1979, pp.11-33.
- 3 Crighton, D.G., and Bashforth, S., "Nonlinear Propagation of Broadband Jet Noise", AIAA Paper AIAA-80-1039, May.1980.
- 4 Howell, G.P. and Morfey, C.L., "Non-linear Propagation of Broadband Noise Signals", *Journal of Sound and Vibration*, Vol. 114, No.2, 1987, pp. 189-201.
- 5 Menounou, P. and Blackstock, D.T., "A New Method to Predict the Evolution of the Power Spectral Density for a Finite Amplitude Sound Wave", *Journal of the Acoustical Society of America*, Vol. 115, No. 2, 2004, pp. 567-580.
- 6 Hamilton, M.F. and Blackstock, D.T., eds., *Nonlinear Acoustics*, Academic, San Diego, 1998.
- 7 Petitjean, B.P. & McLaughlin, D.K., "Experiments on the Nonlinear Propagation of Noise from Supersonic Jets", AIAA Paper 2003-3127, May 2003.



- 8 Bass, H.E., Sutherland, L.C., Zuckerwar, A.J., Blackstock, D.T., Hester, D.M.,  
“Atmospheric Absorption of Sound: Further Developments”, *Journal of the Acoustical Society of America*, Vol.97, No.1, 1995, p.680.
- 9 Bass, H.E., Sutherland, L.C., Zuckerwar, A.J., Blackstock, D.T., Hester, D.M., “Erratum:  
Atmospheric Absorption of Sound: Further Developments”, *Journal of the Acoustical Society of America*, Vol.99, No.2, 1996, p.1259.